

Self-Adaptive Forecasting for Improved Deep Learning on Non-Stationary Time-Series

Sercan Ö. Arik, Nathanael C. Yoder, Tomas Pfister

Google Cloud AI Sunnyvale, CA

Abstract

Real-world time-series datasets often violate the assumptions of standard supervised learning for forecasting – their distributions evolve over time, rendering the conventional training and model selection procedures suboptimal. In this paper, we propose a novel method, Self-Adaptive Forecasting (SAF), to modify the training of time-series forecasting models to improve their performance on forecasting tasks with such non-stationary time-series data. SAF integrates a self-adaptation stage prior to forecasting based on ‘backcasting’, i.e. predicting masked inputs backward in time. This is a form of test-time training that creates a self-supervised learning problem on test samples before performing the prediction task. In this way, our method enables efficient adaptation of encoded representations to evolving distributions, leading to superior generalization. SAF can be integrated with any canonical encoder-decoder based time-series architecture such as recurrent neural networks or attention-based architectures. On synthetic and real-world datasets in domains where time-series data are known to be notoriously non-stationary, such as healthcare and finance, we demonstrate a significant benefit of SAF in improving forecasting accuracy.

Keywords: Time-series, forecasting, non-stationary, self-supervised learning, test-timetraining

2022 MSC: 00-01, 99-00

1. Introduction

Time-series forecasting plays a crucial role in many domains, including finance, healthcare, retail and environmental sciences. Traditional approaches for time-series forecasting are typically based on statistical models, such as ARIMA and its extensions [18, 4], which are recently being outperformed and replaced by high-capacity deep neural networks (DNNs), such as DeepAR [29], MQRNN [33], N-BEATS [26], Informer [35] and TFT [23].

A prominent challenge for time-series forecasting is that many real-world time-series datasets are inherently non-stationary, i.e. their distributions drift over time (see Fig. 1). It is considered one of the key challenges in forecasting on real-world data [22]. Non-stationary behaviors can be trends, cycles, random walks,

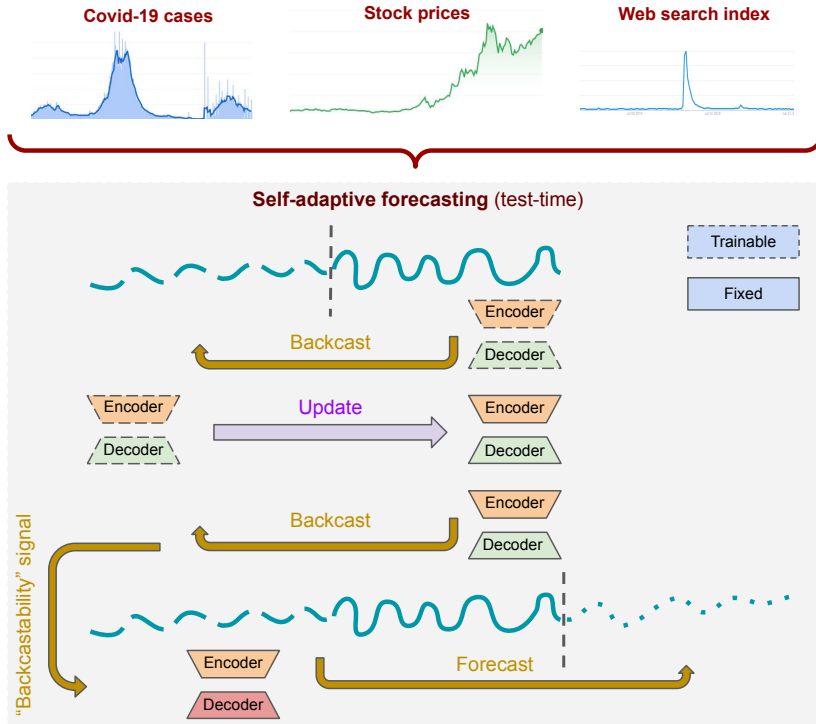


Figure 1: Real-world time-series data from healthcare, finance and the web are often inherently non-stationary, i.e. their distributions drift over time, which renders accurate forecasting challenging. We propose Self-Adaptive Forecasting (SAF), which employs backcasting as form of test-time training to update the encoders and decoders based on self-supervision and a ‘backcastability’ error signal. SAF is composed of an encoder (in orange), as well as a backcast decoder (green) and a forecast decoder (red). By adapting the model at test time according to information learned from the self-supervised loss, a test sample-specific forecasting model is learned which can adapt to non-stationary conditions effectively. We show that SAF improves forecasting accuracy and generalization on a diverse set of datasets, with especially large improvements for highly non-stationary time-series data (shown in Fig. 4).

or combinations of them. Standard supervised learning assumes that training, validation and test datasets come from the same distribution, and each sample is independently and identically distributed [15]. For non-stationary time-series data, however, these assumptions can be severely violated [21]. Consequently, the standard way of applying supervised training, used in most DNN-based time-series methods, is often suboptimal for non-stationary time-series data, yielding significant training-validation and validation-test mismatch and being detrimental for usability [24, 22].

If drifts in data distribution were completely unpredictable, there would not be much that could be done beyond improving the general robustness of the model, particularly since DNNs are particularly sensitive to out-of-distribution data [17, 7]. Yet for many real-world time-series data, these drifts occur with certain trends or ‘somewhat predictable’ patterns. For example, in financial markets, there has been a gradual increase in the number of transactions made by trading algorithms over the course of multiple years [14]. While simple machine learning models may have been able to forecast the prices of financial assets a few decades ago, as these signals are exploited by such trading algorithms, the algorithms themselves change the output distributions and cause the models become less accurate. Although there are many other unpredictable dynamics in financial markets, this rise of algorithmic trading is one long term pattern motivating that one should not treat the data from 1980s and 2010s in the same way. Retail is another domain where there are evolving long term dynamics, such as fashion demand cycles [30]. Non-stationarity is also common in healthcare, where long term patterns in increasing obesity can shape the demand for drugs or treatments that may be related to diseases that are impacted by excessive body fat [1].

If there are time-varying features available that represent the factors causing the drift (such as the day of the year, fashion trend indicator, Covid-19 severity, quantitative trading penetration ratio, or public health indicators), they can be used as exogenous covariates input to the models as in [23] so that the model can learn accurate conditional distributions based on these signals. However, in practice it is often the case that the covariates cannot fully capture all the distribution shifts along time. Therefore it would be strongly desirable to be able to implicitly learn such changes and relate to exogenous signals whenever possible.

In this paper, our goal is to propose a canonical learning system that can effectively learn how to generate accurate forecasts for non-stationary time-series datasets. We propose a new architecture-agnostic method for forecasting non-stationary time-series, Self-Adaptive Forecasting (SAF), which allows forecasting models to better adapt to current dynamics (see Fig. 1). Our proposed method is based on test-time training, which is motivated by the realization that since test samples give a hint about the underlying test distribution, it makes sense to adapt the model at test time according information learned from the test samples. Self-supervision can be used to learn a test-sample specific model that is used to make the final prediction. In SAF, encoded representations are updated with a backcasting self-supervised objective for the task of predicting the masked portion

of the time-varying input features backwards in time. With this adaptation step, the representations are encouraged to fit to the current joint distribution of the inputs accurately. If there are certain trends changing over time, the representations are encouraged to fit the current state. By better reflecting the current state of the varying distribution to condition the generated forecasts (and by having an end-to-end training procedure matching this objective), SAF significantly improves the forecasting accuracy, especially so for datasets with varying dynamics.

We make the following contributions:

1. We propose a novel method to modify the training of time-series forecasting models to improve their performance on non-stationary tasks using inspiration from test-time training. To our knowledge, our work is the first application of test-time training for time-series data and for forecasting.
2. SAF can be integrated into any encoder-decoder based DNN architecture for multi-horizon forecasting, and we demonstrate its efficacy with LSTM Seq2Seq and the attention-based Temporal Fusion Transformer (TFT) [23].
3. We specifically focus on synthetic and real-world datasets that suffer from severe non-stationarity, and demonstrate significant performance improvements with SAF across various cases with different dataset characteristics.

2. Related work

Forecasting non-stationary time-series: Various statistical estimation and machine learning methods have been proposed for non-stationary time-series forecasting, often based on integrating an adaptive component in traditional supervised learning formulations. One approach is modifying the estimation procedure for autoregressive processes with time-varying coefficients [9]. [5] studies Gaussian process models using a non-stationary covariance function. [25] proposes a spectral decomposition procedure, based on the exploitation of recursive smoothing algorithms, for self-adaptive implementation of state-space forecasting and seasonal adjustment. [6] modifies support vector machines using an exponentially increasing regularization constant and an exponentially decreasing tube size to deal with structural changes in the data. [21, 22] proposes a convex learning objective with learning guarantees for the general case of non-stationary non-mixing processes. [28] studies wavelet decomposition-based approaches, which are flexible in modeling local spectral and temporal information that allows capturing short duration, high frequency, longer duration, and lower frequency information simultaneously. Overall, these previous works are model-dependent and are not straightforward to integrate with deep learning.

Deep learning under distribution shift: Numerous works have demonstrated [27, 8, 20] that DNNs can severely suffer as the test distributions deviate from training distributions. Various methods have been proposed to mitigate such performance degradation, particularly for visual data. Domain-adversarial deep learning [12] is one common approach for visual data that encourages the emergence of features that are discriminative for the main learning task on the source domain and indiscriminate with respect to the shift between the domains.

[19] adapts this by optimizing a metric which explicitly models the intra-class domain discrepancy and the inter-class domain discrepancy. [10] proposes dynamic importance weighting which contains estimation of the test-over-training density ratio and fitting the classifier from weighted training data, showing promising results on image classification tasks. In general, the methods in this space are not designed to utilize the time component along distribution shift and they are often not implemented in online fashion (i.e. they expect the test distribution at test time). Therefore, such methods are not commonly used for time-series forecasting. To significantly improve results in non-stationary time-series forecasting with DNNs, a method that explicitly uses the time component along distribution shift would be beneficial.

Test-time training: Test-time training is motivated by the realization that test samples give a hint about the test distribution, as a form of one sample learning. Instead of anticipating the test distribution at training time (as in domain adaptation), the idea is to instead adapt the model at test time according information learned from the test samples. In practice this is achieved by creating a self-supervised objective function that is optimized both at training and testing time. At training time, the self-supervised and supervised losses are optimized jointly, mimicking the testing time scenario. At testing time, the self-supervised loss is optimized on test samples using gradient descent, and the test sample-specific model is used to make the final prediction. [31] demonstrated its benefits for improving image classification accuracy particularly under distribution shifts, using rotation prediction as the self-supervised objective. Beyond simply using multi-task learning, [3] proposes to modify training with gradient-descent based meta learning [11] to better mimic the test-time adaptation task. Our proposed training methods follow the same rationale for applying gradient-descent based meta learning-based training. The test-time training idea has also been adapted to reinforcement learning via self-supervised policy adaptation [16]. To our knowledge, our work is the first application of this concept to time-series data and for forecasting, utilizing the time-component when defining the self-supervised objective and adaptation at test time.

3. Principles behind self-adaptive forecasting

We propose to modify deep learning based forecasting to address the bottlenecks for non-stationarity time-series data, particularly to minimize the impact of distribution mismatch and utilize the predictable patterns in the evolution of distributions. Fig. 2 overviews the general idea of the proposed Self-Adaptive Forecasting (SAF). The desiderata of SAF are listed below:

1. Conditioning forecasting on the current state: We first start with the motivation that we would like the forecasting to be conditioned not only on input covariates, but also on an abstract notion of ‘state’, which should reflect the data distribution around the prediction time. These ‘states’ should be powerful representations of the time-series data in the encoding window, and the distribution they reflect should be globally meaningful. For example, if a very similar regime is observed in the past, a similar state should be retrieved with

the value corresponding to that past timestep. Such ‘states’ should be learned from data and they should directly affect the forecasts. One idea for obtaining such states is to use explicit representations to condition the models and learn these representations separately. We propose to directly reflect the states with encoder weights that are dynamically updated so that they efficiently represent the state of the data in a given window.

2. Test-time training for determining the current state: Determining the states should be done in a ‘self-supervised’ way as the information for future timesteps, the target, would be unknown at test time. We propose to modify the forecasting operation using representations obtained by self-supervised learning at test time. Our modification is based on applying a gradient-descent update with the self-supervised objective. In contrast to learning methods that modify the loss function only during training, such as multi-task learning or autoencoding, test-time training has a loss function for test time (see Fig. 1), which helps to adapt the model to different conditions effectively.

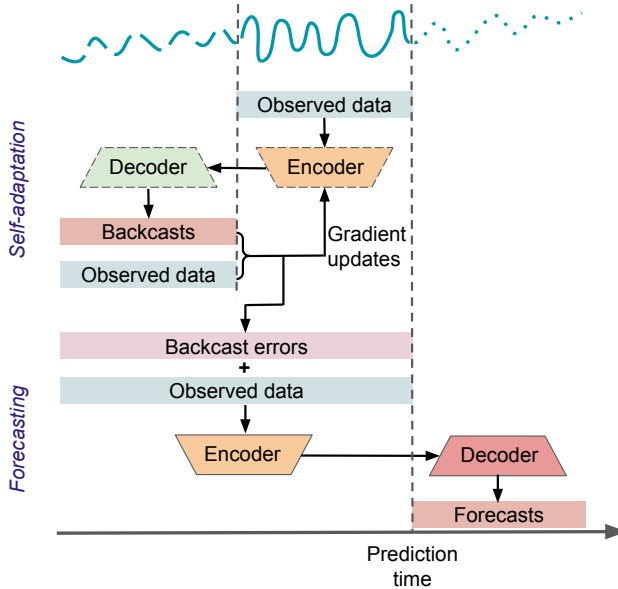


Figure 2: Proposed Self-Adaptive Forecasting (SAF) at test-time to improve deep learning based time-series forecasting by learning to better adapt to current dynamics using self-supervision. During the test-time self-adaptation stage, a masked portion of the input is backcasted (predicting the past), and the gradients of the backcasting loss are used to adapt the encoder (the dashed box denotes it being trainable initially and then the solid box denotes it being used in feed-forward way). During the forecasting stage, this test window-specific adapted encoder is used together with the backcast errors (which provide a signal of ‘backcastability’) to perform the forecast.

3. Meaningful self-supervised learning: It is critical that the self-supervised learning task should be meaningful for the time-series data so that the model can extract the most powerful representation for the forecasting

task. One path is to propose a self-supervised learning task given the domain knowledge (analogous to rotation prediction for object-centric images [31]) – for example, pitch prediction could be a meaningful task for speech time-series data [13]. Instead, to apply our method to wide range of datasets, we propose a canonical self-supervised learning task for forecasting, ‘backcasting’, where the task is to predict the inputs (‘back in time’) in a masked portion of the window. Our motivation for backcasting is based on the intuition that as the past-future relationship evolves along time, the predictability of the relationship at different consecutive timesteps should reflect the evolution. An unexpected event that deteriorates the validity of the learned past-future relationship should show up in the achievable backcasting, as well as achievable forecasting. The backcasting loss metric can be similar to the forecasting loss metric, such as L1 or L2 regression losses. In contrast to the core forecasting task where one often only needs to predict one target covariate (e.g. sales for retail demand forecasting), the self-supervised backcasting cast can benefit from being applied to all input covariates (e.g. number of customers, economical indices, weather etc.) to better learn varying distributions that jointly modeling all covariates.

4. Self-supervised error signal: If there is a large amount of change in the distribution and the current state is very unpredictable, the forecaster component should know about it so that it can adjust accordingly. For example, the forecaster can output more typical values rather than an outlier in the presence of such unpredictable scenarios. To that end, we propose to input the error signal from the self-supervised learning adaptation. We keep the use of this error signal as optional – whether to use it or not is a hyperparameter and picked based on the validation metric.

In the next section, we describe our specific implementation that utilizes conventional building blocks and optimization methods built on these principles.

4. Implementation

Let’s consider the multi-horizon forecasting task of predicting $y[t+1 : t+h]$ from the observed inputs $x[t-m+1 : t]$, where h is the forecasting horizon and m is the input window length.¹ We focus on a canonical multi-horizon forecasting architecture with an encoder $e(\cdot; \Omega_e)$, and forecast decoder $d^{(f)}(\cdot; \Omega_{d(f)})$. In addition to these two modules, SAF requires a backcast decoder $d^{(b)}(\cdot; \Omega_{d(b)})$. The architecture of the backcast decoder can be similar to a forecast decoder as it maps the encoded representations at the corresponding timesteps to backcasts, similar to how the forecasting decoder maps the corresponding timesteps to forecasts. For example, LSTM sequence-to-sequence models [32] can employ separate LSTMs as the encoder, forecasting decoder and backcasting decoders, and the encoded representation can be used as an input to the decoders via the initial state. In contrast, attention-based models such as TFT [23] can contain a self-attention module in the encoder (along with temporal representation

¹[\cdot, \cdot] assumes inclusion of the boundary values.

Algorithm 1 Inference for proposed Self-Adaptive Forecasting (SAF).

Require: Input instance x , encoder $e(\cdot; \Omega_e)$, backcast decoder $d^{(b)}(\cdot; \Omega_{d^{(b)}})$, forecast decoder $d^{(f)}(\cdot; \Omega_{d^{(f)}})$, prediction time t , mask length n , and input window length m .

- 1: $\Theta = \text{Tile}(x[t-m+n+1])$ \triangleright Tile the last element of the unmasked window.
- 2: $\mathbf{r} = e([\Theta, x[t-m+1 : t-m+n] \cup \mathbf{0}; \Omega_e])$ \triangleright Obtain encoded representation for the input window.
- 3: $b = d^{(b)}(\mathbf{r}; \Omega_{d^{(b)}})$ \triangleright Obtain backcasts for the masked window.
- 4: $\Omega_e^{(m)} \leftarrow \Omega_e - \alpha \cdot \nabla_{\Omega_e} L(b, x[t-m+1 : t-m+n])$ \triangleright Self-adaptation: Update the encoder with backcast loss.
- 5: $\Omega_{d^{(b)}}^{(m)} \leftarrow \Omega_{d^{(b)}} - \alpha \cdot \nabla_{\Omega_{d^{(b)}}} L(b, x[t-m+1 : t-m+n])$ \triangleright Self-adaptation: Update the backcast decoder with backcast loss.
- 6: $\mathbf{r} = e(x[t-m+1 : t] \cup \mathbf{0}; \Omega_e^{(m)})$ \triangleright Obtain encoded representation for the entire input window.
- 7: $b = d^{(b)}(\mathbf{r}; \Omega_{d^{(b)}}^{(m)})$ \triangleright Obtain backcasts for the masked window.
- 8: $\mathbf{e} = b - x[t-m+1 : t-m+n]$ \triangleright Obtain errors for the backcasts.
- 9: $\mathbf{r} = e(x[t-m+1 : t-m+n] \cup \mathbf{e}; \Omega_e^{(m)})$ \triangleright Obtain encoded representation for the input window combined with the errors.
- 10: $\hat{y} = d^{(f)}(\mathbf{r}; \Omega_{d^{(f)}}^{(m)})$ \triangleright Forecast.

learning), and decoders can be multi-layer perceptrons (MLPs) that map the encoded representations of the timesteps to the backcasts or forecasts. There is no restriction in the encoder and decoder architectures – they can contain other types of layers, such as convolutional or relational.

We first describe the details of the inference procedure, overviewed in Algorithm 1. To adapt to the evolving distributions, we utilize encoded representations \mathbf{r} to represent the current ‘states’ of the time-series. \mathbf{r} is obtained based on the proposed self-supervised learning task of backcasting, for which we propose masking a portion of the input in the encoded window, and predicting the masked portion with the unmasked portion. For masking, the elements from the hidden portion of the input $x[t-m+1 : t-m+n]$ are replaced with the last observed element of the unmasked portion $x[t-m+n+1]$ (as opposed to naively inputting an arbitrary constant that may change covariate shift for the DNN) (Alg. 1, Step 1 - here *Tile* operation corresponds to constructing the vector with repeated elements). In our experiments, we simply mask half of the window, i.e. $n = m/2$, as it is observed as a reasonable choice across various datasets. n/m ratio can also be treated as a hyperparameter.

The encoded representation \mathbf{r} is input to the backcasting decoder, which produces the backcasts \mathbf{b} to be used in the loss $L(\mathbf{b}, x[t-m+1 : t-m+n])$. The loss is used to supervise the encoder and backcast decoder based on a single-step gradient descent update (Alg. 1, Steps 4 and 5) – i.e. they are adapted to more accurately backcast the input. Each inference run modifies the pre-trained encoder $e(\cdot; \Omega_e^{(m)})$ (Alg. 1, Step 4) and backcast decoder $d^{(b)}(\cdot; \Omega_{d^{(b)}}^{(m)})$

(Alg. 1, Step 5) with the gradient descent updates. To ensure that the original pre-trained model is not altered between different inference runs and the model outputs do not change for multiple applications of the same model, we apply them to a different copy of weights (denoted with the $^{(m)}$ superscript).

After the self-adaptation update, the encoded representations \mathbf{r} are re-obtained with the updated encoder $e(\cdot; \Omega_e^{(m)})$ (Alg. 1, Step 6). In addition, we also re-obtain the backcasts and estimate the backcasting error \mathbf{e} (Alg. 1, Steps 7 and 8) with the goal of providing useful signal on the difficulty of prediction of a particular timestep, which is a useful signal to indicate the level of non-stationarity. We propose to use this backcasting error \mathbf{e} in the encoder as an additional time-varying feature (appended to as a new feature) along with the input in the entire time window. The forecasts are obtained from the encoded representation and the error signal, $\mathbf{r} = e(x[t - m + 1 : t - m + n] \cup \mathbf{e})$. If used, error values are simply concatenated for the timesteps wherever they exist to be input into the encoder architecture, otherwise $\mathbf{0}$ are used. Note that we do not have the backcasting error for the encoder for backcasting, so we instead input $\mathbf{0}$ (Alg. 1, Steps 2 and 6). Finally, the forecasting decoder generates the multi-horizon forecasts as the outputs (Alg. 1, Step 10) using the updated encoded representations.

For training, matching the inference procedure is important. Our goal is to learn the encoder $e(\cdot; \Omega_e)$, backcast decoder $d^{(b)}(\cdot; \Omega_{d^{(b)}})$, forecast decoder $d^{(f)}(\cdot; \Omega_{d^{(f)}})$ from the training split of the time-series data, with the end goal of optimizing for the actual test-time functionality given in Algorithm 1. We propose to match the Algorithm 1 similarly during training, to obtain the forecasting loss, which is used to update the encoder and forecasting decoder. This training method is applicable even with batches containing different entities and prediction timesteps, as they have an encoding window of certain duration. Samples from different prediction timesteps, as well as the samples from different entities, can be combined in the same batch for computational efficiency during training. The full training procedure is shown in the Appendix.

5. Forecasting performance

We perform experiments on various non-stationary time-series datasets to evaluate the efficacy of the proposed SAF. Our method is model architecture agnostic, and we demonstrate its potential with an LSTM sequence-to-sequence model and an attention-based model, TFT. For the LSTM sequence-to-sequence model, the backcast decoder $d^{(b)}(\cdot; \Omega_{d^{(b)}})$ is based on another LSTM. Static features are mapped with an MLP, and the static representations are either added or concatenated to the encoded representations coming from the LSTM (the choice is treated as a hyperparameter, see the Appendix). For TFT, it is based on a dense layer that maps the prediction from attention outputs, in the same way that the dense layer in standard TFT maps the attention outputs to forecasts. Some datasets contain multiple entities (i.e. multiple target time-series). For all experiments, we consider datasets with training-validation-test

split over time. Model selection is based on the validation performance, and we evaluate the test performance. The overall goal is to compare conventional application of time-series forecasting to SAF. Please see the Appendix for further details datasets and training.

Table 1: Test MSE on the 4 synthetic autoregressive processes datasets, averaged over 11 different durations (with \pm standard deviations for the aggregate statistics over different time-series durations). For all cases, the hyperparameters are picked based on the validation MSE. A significant improvement is observed on the two non-stationarity datasets (AR1& AR3) with up to $\sim 10\%$ reduction for average MSE.

	AR1	AR2	AR3	AR4
LSTM Seq2Seq	.002601 \pm .000822	.001370 \pm .000750	.002061 \pm .001338	.001167 \pm .000159
LSTM Seq2Seq - SAF	.002550 \pm .000718 (-1.97%)	.001319 \pm .000692 (-3.73%)	.001859 \pm .000616 (-9.81%)	.001185 \pm .000181 (1.54%)
TFT	.002744 \pm .000821	.001416 \pm .000841	.001823 \pm .000815	.001206 \pm .000180
TFT - SAF	.002540 \pm .000729 (-7.44%)	.001426 \pm .000881 (0.70%)	.001659 \pm .000525 (-9.00%)	.001164 \pm .000171 (-3.49%)

Table 2: Properties of the real-world datasets used in experiments. Details are provided in Appendix.

	Covid-19	M5	Electricity	Crypto	SP500
Sampling frequency	Daily	Daily	Hourly	Minutely	Daily
Number of entities	56	200	369	14	75
Forecasting horizon	28	28	24	1	1
Number of time-varying features	20	13	9	8	6
Number of static features	15	5	2	3	1
Number of train timesteps	283	1707	5471	1.9M	2074
Number of validation timesteps	14	14	168	2160	30
Number of test timesteps	14	14	168	2160	30

5.1. Synthetic datasets

We consider 4 autoregressive random processes from [22] with additive Gaussian noise ϵ_t (with a mean of 0 and standard deviation of .03):

AR1: Abrupt changes in the data generating mechanism: $y[t] = \alpha[t] \cdot y[t-1] - \epsilon_t$, where $\alpha[t] = -0.9$ for $t \in [1000, 2000]$ and 0.9 otherwise.

AR2: Parameters of the data generating process smoothly drifting: $y[t] = \alpha[t] \cdot y[t-1] - \epsilon_t$, where $\alpha[t] = 1 - (t/1500)$.

AR3: Parameter changes occurring at random times : $y[t] = \alpha[t] \cdot y[t-1] - \epsilon_t$, where $\alpha[t]$ is either -0.5 or 0.9 based on the stochastic process, which after spending τ last time steps, at the next time step will stay in the same one with probability $(0.99995)^\tau$ and will move to the different state with probability $1 - (0.99995)^\tau$.

AR4: With stationarity: $y[t] = -0.5 \cdot y[t-1] - \epsilon_t$.

We consider 11 different total dataset durations in the range [1000, 3000] with increments of 200, and a forecasting horizon of $h = 5$. We use validation and test durations of 100 for each case and the rest of the data is used for training.

Mean squared error (MSE) loss is used for training and evaluation (given the additive noise has Gaussian distribution).

Table 1 shows the results on these 4 datasets. We observe the benefit of SAF with both LSTM Seq2Seq and TFT models, especially on the two non-stationarity datasets (AR1 & AR3) with up to $\sim 10\%$ reduction for average MSE. On AR2, the benefit is smaller for LSTM Seq2Seq, and we observe slight underperformance for TFT. On AR4, the stationary dataset, SAF gives slightly worse results than the baseline, which we attribute to distracting the model capacity with the self-supervised task when the supervised task itself is too simple for model to learn across available data.

5.2. Real-world datasets

We consider the real-world time-series datasets from Healthcare, Retail, Energy and Finance domains. We intentionally picked datasets with different characteristics (summarized in Table 2) to demonstrate the applicability of SAF across different regimes. The Appendix contains additional details about the datasets.

Covid-19: We consider the task of forecasting the Covid-19 deaths for the next 28 days at state-level granularity from various time-varying and static covariates as in [2].

M5: We use the M5 competition dataset² for the task of forecasting the unit sales of retail goods.

Electricity: We consider the task of forecasting electricity consumption of different customers on the UCI Electricity Load Diagrams dataset [34].

Crypto: We use the G-Research Crypto Forecasting dataset³ for the task of forecasting short term returns in 14 popular cryptocurrencies given the prediction targets of the competition.

SP500: We consider the task of forecasting the daily returns at open for 75 equities from SP500 index (which have data since 01-01-2012) using Kaggle’s ‘Stock Market Data’⁴.

Table 3: Test set results on the real-world datasets. The metrics are in MAE except M5 and Crypto, for which we use MSE (following the metric choices of related literature for these problems). For all cases, the hyperparameters are picked based on the validation metric. SAF provides consistent improvements with both LSTM Seq2Seq and TFT across all datasets.

	Covid-19	M5	Electricity	Crypto	SP500
LSTM Seq2Seq, baseline	1357.1	5.741	45.95	3.592	0.6836
LSTM Seq2Seq, SAF	793.5 (-41.6%)	5.474 (-4.6%)	44.53 (-3.6%)	3.459 (-3.8%)	0.6656 (-2.7%)
TFT, baseline	1394.7	5.817	43.10	4.249	0.6693
TFT, SAF	1117.9 (-19.9%)	5.609 (-3.6%)	40.89 (-5.4%)	3.459 (-18.6%)	0.6689 (-0.1%)

Table 3 shows the test set results on the above real-world datasets for both LSTM Seq2Seq and TFT-based architectures. Overall, we observe consistent

²<https://www.kaggle.com/c/m5-forecasting-accuracy/>

³<https://www.kaggle.com/c/g-research-crypto-forecasting/>

⁴<https://www.kaggle.com/paultimothymooney/stock-market-data>

improvement with SAF with both LSTM Seq2Seq and TFT across all datasets, with some variance in improvement depending on the dataset. We observe the largest accuracy improvement on Covid-19, with $> 40\%$ error reduction for LSTM Seq2Seq, and $> 19\%$ for TFT. There are some characteristics of the Covid-19 dataset that can particularly benefit SAF: (i) potential higher non-stationarity in the dynamics as noted by different studies on the pandemic [2] (given the rapid changes in the disease dynamics caused by non-pharmaceutical interventions – e.g. mask mandates or school closures), vaccination and virus mutations); (ii) the small size of the dataset and skewed feature distributions, resulting in conventional models getting stuck to a local optima quickly; and (iii) the existence of more consistent learnable patterns via backcasting (e.g. cumulative deaths being monotonic and increasing with a rate in a certain interval). After Covid-19, the biggest improvement is observed for the Crypto dataset, which is also known to possess high non-stationarity in its dynamics [?]. The dataset on which we show the smallest improvement, SP500, tends to yield similar results with different models and hyperparameters, which we attribute to limited predictability of the target.

6. Performance analyses

In this section, we shed further light on how SAF is helping for improving the forecasting accuracy.

Robust hyperparameter selection: One of the benefits of SAF is that it is able to reduce the mismatch between validation test metrics which helps select a better model. Fig. 3 shows the validation and test results for the individual hyperparameter trials. As can be observed, the validation and test correlation improves especially in the regime of low validation error trials, which is practically valuable as performing extensive hyperparameter searches can be expensive. For example, the Spearman’s rank correlation coefficient is 0.706 for the LSTM Seq2Seq baseline without SAF vs. 0.775 with SAF when the trials with validation MAE less than 800 are considered from Fig. 3. This enables improved hyperparameter optimization without expensive cross-validation approaches.

Forecast improvement scenarios: Fig. 4 exemplifies the cases where the forecasts are improved significantly on Covid-19. We observe that SAF provides a considerable improvement in learning the overall trend behavior accurately and preventing unrealistic exponential growth, a typical problem suffered by autoregressive models for multi-horizon prediction. In addition, in some cases it helps learning the initial forecasting point more accurately, i.e. it discovers the knowledge that Covid-19 cumulative deaths on the first prediction date should not be significantly different than the last observed cumulative value. Note that such knowledge is not embodied in the black-box LSTM architecture and the model needs to learn it from a small amount of training data. The inductive bias coming from SAF seems to be helping with this, as the backcasting task also provides supervision to learn the continuity of the cumulative quantities.

Number of time-varying features: Although the core forecasting task focuses on predicting one target covariate, the self-supervised backcasting can

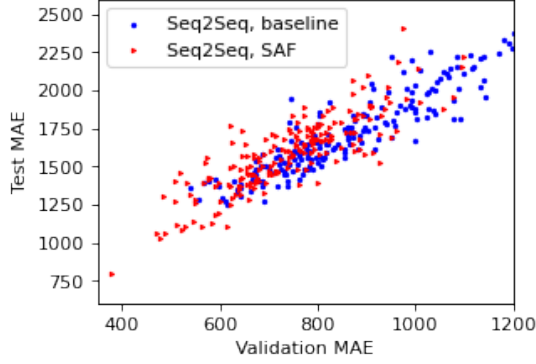


Figure 3: Validation vs. test MAE for different hyperparameter trials (each marker corresponds to a different set of hyperparameter configurations) for LSTM Seq2Seq on Covid-19. The proposed SAF can improve both the achievable validation performance and the validation and test correlation across runs.

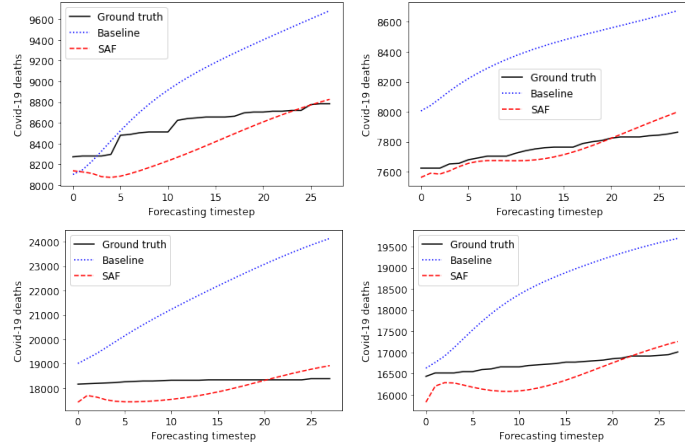


Figure 4: Ground truth and multi-horizon daily forecasts with LSTM Seq2Seq on Covid-19 datasets for 4 US states, without (blue) and with (red) SAF.

benefit from being applied to all input time-varying covariates. We observe that on the datasets with a high number of time-varying covariates (see Table 2), particularly Covid-19, we tend to observe bigger benefit of SAF. As time-series datasets are containing more and more covariates (given the corresponding data infrastructures are becoming more widely available to join many relevant time-series signals), they are positioned for superior time-series forecasting by adapting SAF.

Ablation studies: Table 4 demonstrates the importance of having the gradient-descent based update steps in self-adaptation stages for encoder (Alg. 1, Step 4) and decoder (Alg. 1, Step 5) as well as using the self-supervised error signal (given in Alg. 1, Step 8), as core constituents of SAF.

Table 4: Ablation studies on Covid-19 with LSTM Seq2Seq.

Ablation	Test MAE
SAF without updating the decoder	1421.1
SAF without updating the encoder	1157.7
SAF without error signal	941.2
SAF	793.5

7. Conclusions

In this paper, we propose self-adaptive forecasting (SAF), a novel approach to time-series forecasting to improve deep learning performance on non-stationarity time-series data. SAF integrates a self-adaptation stage prior to forecasting based on ‘backcasting’ the masked inputs, a form of test-time training. This enables adapting encoded representations efficiently to evolving distributions, resulting in better generalization and more robust hyperparameter selection. SAF can be integrated with any canonical encoder-decoder based time-series forecasting model such as recurrent neural networks or attention-based architectures. On various non-stationary time-series datasets with distinct characteristics, we show that SAF results in significant improvements in forecasting accuracy. We believe SAF can open new horizons on how to design learning methods for time-series forecasting.

8. Appendix

Algorithm 2 Training for proposed self-adaptive forecasting.

Require: Training dataset $S = \{(x, y)\}$; encoder $e(\cdot; \Omega_e)$, backcast decoder $d^{(b)}(\cdot; \Omega_{d^{(b)}})$, forecast decoder $d^{(f)}(\cdot; \Omega_{d^{(f)}})$, mask length n , and input window length m .

- 1: **while** Until convergence **do**
- 2: $(x_B, y_B) \in S$ ▷ Sample a batch.
- 3: $\Theta_B = \text{Tile}(x_B[t-m+n+1])$ ▷ Tile the last element of the unmasked window.
- 4: $\mathbf{r}_B = e([\Theta_B, x_B[t-m+1 : t-m+n]] \cup \mathbf{0}; \Omega_e)$ ▷ Obtain encoded representation for the masked input window.
- 5: $\mathbf{b}_B = d^{(b)}(\mathbf{r}_B; \Omega_{d^{(b)}})$ ▷ Obtain backcasts for the masked window.
- 6: $\Omega_e \leftarrow \Omega_e - \alpha \cdot \nabla_{\Omega_e} L(\mathbf{b}_B, x_B[t-m+1 : t-m+n])$ ▷ Self-adaptation: Update the encoder with the backcast loss.
- 7: $\Omega_{d^{(b)}} \leftarrow \Omega_{d^{(b)}} - \alpha \cdot \nabla_{\Omega_{d^{(b)}}} L(\mathbf{b}_B, x_B[t-m+1 : t-m+n])$ ▷ Self-adaptation: Update the decoder with the backcast loss.
- 8: $\mathbf{r}_B = e(x[t-m+1 : t] \cup \mathbf{0}; \Omega_e)$ ▷ Obtain encoded representation for the entire input window.
- 9: $\mathbf{b}_B = d^{(b)}(\mathbf{r}_B; \Omega_{d^{(b)}})$ ▷ Obtain backcasts for the masked window.
- 10: $\mathbf{e}_B = \mathbf{b}_B - x_B[t-m+1 : t-m+n]$ ▷ Obtain errors for the backcasts.
- 11: $\mathbf{r}_B = e(x_B[t-m+1 : t] \cup \mathbf{e}_B; \Omega_e)$ ▷ Obtain encoded representation for the input window combined with the errors.
- 12: $\hat{y}_B = d^{(f)}(\mathbf{r}_B; \Omega_{d^{(f)}})$ ▷ Forecast.
- 13: $\Omega_e \leftarrow \Omega_e - \gamma \cdot \nabla_{\Omega_e} L(\hat{y}_B, y_B)$ ▷ Update the encoder with the forecast loss.
- 14: $\Omega_{d^{(f)}} \leftarrow \Omega_{d^{(f)}} - \gamma \cdot \nabla_{\Omega_{d^{(f)}}} L(\hat{y}_B, y_B)$ ▷ Update the decoder with the forecast loss.

8.1. Pseudo-code for training

Algorithm 2 shows the pseudocode for training for the proposed SAF.

8.2. Dataset and hyperparameter tuning details

For all datasets, we use automated hyperparameter tuning based on the validation performance. For synthetic autoregressive datasets we use 100, for other datasets we use 200 trials. Tables 5 show the hyperparameter search spaces used for all datasets.

Autoregressive processes: Table 5 shows the hyperparameter search space used in experiments.

Covid-19: We adapt the data from [2]. The datasets consist 391 days from the start date of March 1, 2020. We use the last 14 days for testing and the preceding 14 for validation. Static features include ‘population’, ‘income per capita’, ‘population density per sq km’, ‘number of households with public

Table 5: Hyperparameter search space for synthetic autoregressive datasets.

Hyperparameter	Candidate values
Batch size	[32, 64, 128, 256]
Baseline learning rate	[.0001, .0003, .001]
Self-adaptation learning rate (for SAF only)	[.00003, .0001, .0003, .001]
Number of units	[16, 32, 64]
Number of attention heads (for TFT only)	[1, 2]
Dropout keep probability (for TFT only)	[0.5, 0.8, 1.0]
Encoder window length	[10, 30, 50]
Representation combination	[Additive, Concatenation]
Max. number of iterations	3000
Use of backcasting errors (for SAF only)	[True, False]

assistance or food stamps', '-60 population', 'number of icu beds', 'number of households', 'number of hospitals with ratings 1-5', 'air quality', 'number of hospitals with non-emergency/emergency services and acute care and critical access', 'hospital ratings with above/below national average'. Time-varying features include 'number of deaths, cases, recovered, hospitalized, in ICU, and on ventilator', 'mobility indices', 'total tests', 'social distancing indicators for restaurants and bars, non essential businesses, general population stay at home, school closures, mass gathering, face mask restrictions and emergency declarations', 'day of the week', 'max/min/mean temperature', 'rainfall and snowfall', 'antibody and antigen test counts', 'search indices for symptoms cough, chills, anosmia, infection, chest pain, fever and shortness of breath', and 'vaccination counts for one and two doses'. We employ standard normalization to all features with statistics averaged across all entities. Table 6 shows the hyperparameter search space used in experiments.

Table 6: Hyperparameter search space for Covid-19 dataset.

Hyperparameter	Candidate values
Batch size	[64, 128, 256, 512]
Baseline learning rate	[.0001, .0003, .001, .003]
Self-adaptation learning rate (for SAF only)	[.00001, .00003, .0001, .0003, .001]
Number of units	[16, 32, 64, 128, 256]
Number of attention heads (for TFT only)	[1, 2, 4]
Dropout keep probability (for TFT only)	[0.5, 0.8, 0.9, 1.0]
Encoder window length	[10, 30, 50]
Representation combination	[Additive, Concatenation]
Max. number of iterations	10000
Use of backcasting errors (for SAF only)	[True, False]

M5: From the M5 dataset ⁵, we use the time-series for the first 200 products based on the IDs. We employ standard normalization to all features with statistics averaged across all entities. Table 7 shows the hyperparameter search space used in experiments.

Table 7: Hyperparameter search space for M5 dataset.

Hyperparameter	Candidate values
Batch size	[64, 128, 256]
Baseline learning rate	[.0001, .0003, .001, .003]
Self-adaptation learning rate (for SAF only)	[.00003, .0001, .0003, .001]
Number of units	[32, 64, 128, 256, 432]
Number of attention heads (for TFT only)	[1, 2, 4, 8]
Dropout keep probability (for TFT only)	[0.5, 0.8, 0.9, 1.0]
Encoder window length	[20, 50, 100, 150]
Representation combination	[Additive, Concatenation]
Max. number of iterations	60000
Use of backcasting errors (for SAF only)	[True, False]

Electricity: We use the Electricity dataset [34] as is. Similar to [23], we apply per-entity normalization, unlike other datasets. Table 8 shows the hyperparameter search space used in experiments.

Table 8: Hyperparameter search space for Electricity dataset.

Hyperparameter	Candidate values
Batch size	[64, 128, 256, 512, 1024]
Baseline learning rate	[.0001, .0003, .001, .003]
Self-adaptation learning rate (for SAF only)	[.00001, .00003, .0001, .0003, .001]
Number of units	[32, 64, 128, 256]
Number of attention heads (for TFT only)	[1, 2, 4, 8]
Dropout keep probability (for TFT only)	[0.5, 0.8, 0.9, 1.0]
Encoder window length	[96, 168]
Representation combination	[Additive, Concatenation]
Max. number of iterations	100000
Use of backcasting errors (for SAF only)	[True, False]

Crypto: We use the G-Research Crypto Forecasting data on Kaggle⁶, to forecast short term returns in 14 popular cryptocurrencies. The data is since 2018. We scale the given target by 1000. We use all time-varying and static features as is. We employ standard normalization to all features with statistics averaged across all entities.

Table 9 shows the hyperparameter search space used in experiments.

⁵<https://www.kaggle.com/c/m5-forecasting-accuracy/>

⁶<https://www.kaggle.com/c/g-research-crypto-forecasting/>

Table 9: Hyperparameter search space for Crypto dataset.

Hyperparameter	Candidate values
Batch size	[64, 128, 256, 512]
Baseline learning rate	[.00003, .0001, .0003, .001]
Self-adaptation learning rate (for SAF only)	[.00001, .00003, .0001, .0003]
Number of units	[64, 128, 256]
Number of attention heads (for TFT only)	[1, 2, 4]
Dropout keep probability (for TFT only)	[0.5, 0.8, 1.0]
Encoder window length	[60, 120, 240]
Representation combination	[Additive, Concatenation]
Max. number of iterations	[50000, 100000]
Use of backcasting errors (for SAF only)	[True, False]

SP500: We adapt the data from Kaggle ‘Stock Market Data’⁷ From SP500 index, we choose 75 equities as the ones that have data since 01-01-2012: ‘FB’, ‘JKHY’, ‘GOOG’, ‘DVA’, ‘FIS’, ‘LBTYA’, ‘FAST’, ‘LNT’, ‘FE’, ‘ILMN’, ‘DPZ’, ‘ESS’, ‘GM’, ‘JNPR’, ‘FFIV’, ‘EOG’, ‘FANG’, ‘ICE’, ‘DRI’, ‘EQIX’, ‘GWW’, ‘EA’, ‘DHI’, ‘IPGP’, ‘HES’, ‘MKTX’, ‘ABBV’, ‘GILD’, ‘EMN’, ‘FCX’, ‘EW’, ‘KRA’, ‘FN’, ‘DG’, ‘FDX’, ‘FISV’, ‘ENS’, ‘MPC’, ‘EXR’, ‘LVS’, ‘EL’, ‘FRC’, ‘D’, ‘LRCX’, ‘ISRG’, ‘EQR’, ‘CTQ’, ‘EIX’, ‘DXCM’, ‘LNC’, ‘CTSH’, ‘HFC’, ‘KEY’, ‘IT’, ‘HBI’, ‘GPC’, ‘HSY’, ‘FBHS’, ‘DFS’, ‘DAL’, ‘EFX’, ‘GRMN’, ‘KSS’, ‘KMX’, ‘FLT’, ‘FTI’, ‘CUK’, ‘HRL’, ‘ES’, ‘DLTR’, ‘CHTR’, ‘EBAY’, ‘GPN’, ‘DRE’, and ‘CTXS’. We use the time-varying features of ‘Low’, ‘Open’, ‘High’, ‘Close’, and ‘Adjusted Close’ prices, and ‘Volume’, all converted to percent change. We employ standard normalization to all features with statistics averaged across all entities. Table 10 shows the hyperparameter search space used in experiments.

Table 10: Hyperparameter search space for SP500 dataset.

Hyperparameter	Candidate values
Batch size	[32, 64, 128, 256]
Baseline learning rate	[0.0001, 0.0003, 0.001]
Self-adaptation learning rate (for SAF only)	[.00001, .00003, .0001, .0003, .001]
Number of units	[32, 64, 96, 128, 256]
Number of attention heads (for TFT only)	[1, 2, 4, 8]
Dropout keep probability (for TFT only)	[0.5, 0.8, 0.9, 1.0]
Encoder window length	[96, 168]
Representation combination	[Additive, Concatenation]
Max. number of iterations	40000
Use of backcasting errors (for SAF only)	[True, False]

⁷<https://www.kaggle.com/paultimothymooney/stock-market-data>

References

- [1] Afshin, A., Forouzanfar, M., Reitsma, M., Sur, P., Estep, K., Lee, A., Marczak, L., Mokdad, A., Moradi-Lakeh, M., Naghavi, M., Salama, J., Vos, T., Abate, K., Cristiana, A., Ahmed, M., Al-Aly, Z., Alkerwi, A., Al-Raddadi, R., Amare, A., and Collaborators, G. (2017). Health effects of overweight and obesity in 195 countries over 25 years. *New England Journal of Medicine*, 377(1):13–27.
- [2] Arik, S. O., Shor, J., Sinha, R., Yoon, J., Ledsam, J. R., Le, L. T., Dusenberry, M. W., Yoder, N. C., Popendorf, K., Epshteyn, A., Euphrosine, J., Kanal, E., Jones, I., Li, C.-L., Luan, B., Mckenna, J., Menon, V., Singh, S., Sun, M., Ravi, A. S., Zhang, L., Sava, D., Cunningham, K., Kayama, H., Tsai, T., Yoneoka, D., Nomura, S., Miyata, H., and Pfister, T. (2021). A prospective evaluation of ai-augmented epidemiology to forecast COVID-19 in the usa and japan. *npj Digital Medicine*.
- [3] Bartler, A., Bühler, A., Wiewel, F., Döbler, M., and Yang, B. (2021). MT3: meta test-time training for self-supervised test-time adaption. *arXiv:2103.16201*.
- [4] Box, G. E. P. and Pierce, D. A. (1970). Distribution of residual autocorrelations in autoregressive-integrated moving average time series models. *Journal of the American Statistical Association*, 65(332):1509–1526.
- [5] Brahim-Belhouari, S. and Bermak, A. (2004). Gaussian process for non-stationary time series prediction. *Computational Statistics & Data Analysis*, 47(4):705–712.
- [6] Cao, L. and Gu, Q. (2002). Dynamic support vector machines for non-stationary time series forecasting. *Intell. Data Anal.*, 6:67–83.
- [7] Chen, J., Li, Y., Wu, X., Liang, Y., and Jha, S. (2020). Robust out-of-distribution detection for neural networks. *arXiv:2003.09711*.
- [8] Chen, M. F., Goel, K., Sohoni, N. S., Poms, F., Fatahalian, K., and Ré, C. (2021). Mandoline: Model evaluation under distribution shift. *arXiv:2107.00643*.
- [9] Dahlhaus, R. (1997). Fitting time series models to nonstationary processes. *The Annals of Statistics*, 25(1):1 – 37.
- [10] Fang, T., Lu, N., Niu, G., and Sugiyama, M. (2020). Rethinking importance weighting for deep learning under distribution shift. *arXiv:2006.04662*.
- [11] Finn, C., Abbeel, P., and Levine, S. (2017). Model-agnostic meta-learning for fast adaptation of deep networks. *arXiv:1703.03400*.
- [12] Ganin, Y., Ustinova, E., Ajakan, H., Germain, P., Larochelle, H., Laviolette, F., Marchand, M., and Lempitsky, V. (2016). Domain-adversarial training of neural networks. *arXiv:1505.07818*.

- [13] Gfeller, B., Frank, C., Roblek, D., Sharifi, M., Tagliasacchi, M., and Veličković, M. (2020). Spice: Self-supervised pitch estimation. *IEEE Trans Audio, Speech, and Language Processing*, 28:1118–1128.
- [14] Glantz, M. and Kissell, R. (2013). Multi-asset risk modeling: Techniques for a global economy in an electronic and algorithmic trading era. *Multi-Asset Risk Modeling: Techniques for a Global Economy in an Electronic and Algorithmic Trading Era*, pages 1–516.
- [15] Goodfellow, I., Bengio, Y., Courville, A., and Bengio, Y. (2016). *Deep learning*, volume 1. MIT Press.
- [16] Hansen, N., Jangir, R., Sun, Y., Alenyà, G., Abbeel, P., Efros, A. A., Pinto, L., and Wang, X. (2021). Self-supervised policy adaptation during deployment. *arXiv:2007.04309*.
- [17] Hendrycks, D. and Gimpel, K. (2016). A baseline for detecting misclassified and out-of-distribution examples in neural networks. *arXiv:1610.02136*.
- [18] Hillmer, S. C. and Tiao, G. C. (1982). An arima-model-based approach to seasonal adjustment. *Journal of the American Statistical Association*, 77(377):63–70.
- [19] Kang, G., Jiang, L., Yang, Y., and Hauptmann, A. G. (2019). Contrastive adaptation network for unsupervised domain adaptation. *arXiv:1901.00976*.
- [20] Koh, P. W., Sagawa, S., Marklund, H., Xie, S. M., Zhang, M., Balsubramani, A., Hu, W., Yasunaga, M., Phillips, R. L., Beery, S., Leskovec, J., Kundaje, A., Pierson, E., Levine, S., Finn, C., and Liang, P. (2020). WILDS: A benchmark of in-the-wild distribution shifts. *arXiv:2012.07421*.
- [21] Kuznetsov, V. and Mohri, M. (2015). Learning theory and algorithms for forecasting non-stationary time series. In *NIPS*.
- [22] Kuznetsov, V. and Mohri, M. (2020). Discrepancy-based theory and algorithms for forecasting non-stationary time series. *Annals of Mathematics and Artificial Intelligence*, 88(4):367–399.
- [23] Lim, B., Arik, S. O., Loeff, N., and Pfister, T. (2021). Temporal fusion transformers for interpretable multi-horizon time series forecasting. *International Journal of Forecasting*, 37(4):1748–1764.
- [24] Montero-Manso, P. and Hyndman, R. J. (2020). Principles and algorithms for forecasting groups of time series: Locality and globality. *CoRR*, abs/2008.00444.
- [25] Ng, C. N. and Young, P. C. (1990). Recursive estimation and forecasting of non-stationary time series. *Journal of Forecasting*, 9(2):173–204.

- [26] Oreshkin, B. N., Carpov, D., Chapados, N., and Bengio, Y. (2019). N-beats: Neural basis expansion analysis for interpretable time series forecasting. *arXiv:1905.10437*.
- [27] Ovadia, Y., Fertig, E., Ren, J., Nado, Z., Sculley, D., Nowozin, S., Dillon, J. V., Lakshminarayanan, B., and Snoek, J. (2019). Can you trust your model's uncertainty? evaluating predictive uncertainty under dataset shift. *arXiv:1906.02530*.
- [28] Rhif, M., Ben Abbes, A., Farah, I. R., Martínez, B., and Sang, Y. (2019). Wavelet transform application for/in non-stationary time-series analysis: A review. *Applied Sciences*, 9(7).
- [29] Salinas, D., Flunkert, V., Gasthaus, J., and Januschowski, T. (2020). Deepar: Probabilistic forecasting with autoregressive recurrent networks. *International Journal of Forecasting*, 36(3):1181–1191.
- [30] Sproles, G. B. (1981). Analyzing fashion life cycles—principles and perspectives. *Journal of Marketing*, 45(4):116–124.
- [31] Sun, Y., Wang, X., Liu, Z., Miller, J., Efros, A. A., and Hardt, M. (2019). Test-time training for out-of-distribution generalization. *arXiv:1909.13231*.
- [32] Sutskever, I., Vinyals, O., and Le, Q. V. (2014). Sequence to sequence learning with neural networks. *arXiv:1409.3215*.
- [33] Wen, R., Torkkola, K., Narayanaswamy, B., and Madeka, D. (2017). A multi-horizon quantile recurrent forecaster. In *NIPS Workshops*.
- [34] Yu, H.-F., Rao, N., and Dhillon, I. S. (2016). Temporal regularized matrix factorization for high-dimensional time series prediction. In *NIPS*.
- [35] Zhou, H., Zhang, S., Peng, J., Zhang, S., Li, J., Xiong, H., and Zhang, W. (2021). Informer: Beyond efficient transformer for long sequence time-series forecasting. *arXiv:2012.07436*.